

Behavior and prediction of photochemical degradation of chlorinated polycyclic aromatic hydrocarbons in cyclohexane

Takeshi Ohura ^{*}, Takashi Amagai, Masakazu Makino

Institute for Environmental Sciences, University of Shizuoka, 52-1 Yada, Shizuoka 422-8526, Japan

Received 24 April 2007; received in revised form 29 August 2007; accepted 29 August 2007

Available online 23 October 2007

Abstract

The photochemical degradation of 11 chlorinated polycyclic aromatic hydrocarbons (CIPAHs) and the corresponding 5 parent PAHs was examined to simulate the compound's fate on aerosol surfaces. All the CIPAHs and PAHs decayed according to the first-order reaction rate kinetics. The photolysis rates of CIPAHs varied greatly according to the skeleton of PAHs; the rates of chlorophenanthrenes (CIPhes) and 1-chloropyrene were higher than those of corresponding parent PAHs, whereas chlorofluoranthenes, 7-chlorobenz[*a*]anthracene and 6-chlorobenz[*a*]pyrene were more stable under irradiation compared to respective parent PAH. Considering the photoproducts of CIPhes detected, the oxidation could occur immediately at positions of the highest frontier electron density. Finally, the quantitative structure-property relationship models were developed for direct photolysis half-lives and average quantum yields of the CIPAHs and parent PAHs, in which the significant factors affecting photolysis were E_{LUMO+1} , total energy and surface area, and E_{LUMO} , $E_{LUMO} - E_{HOMO}$ and total energy, respectively.
© 2007 Elsevier Ltd. All rights reserved.

Keywords: CIPAH; Photolysis; Half-lives; Quantum yield; QSPR

1. Introduction

Polycyclic aromatic hydrocarbons (PAHs) are ubiquitous hazardous materials because of their mutagenic and carcinogenic properties, and are distributed in the environment through combustion, discharge of fossil fuels, automobile emissions, and subsequent atmospheric transport and deposition (Bidleman, 1988; Baek et al., 1991; Mantz et al., 2005; Lönnemark and Blomqvist, 2006; Pekey et al., 2007). Therefore, determination of the environmental fate of PAHs is important for human risk assessment (Menzie et al., 1992; Finlayson-Pitts and Pitts, 1997; Sabljic, 2001). The dominant degradation pathway of PAHs associated to graphitic particles in the atmosphere is suggested to be photolysis (Nielsen, 1984; Kamens et al., 1988; McDow et al., 1994; Finlayson-Pitts and Pitts, 1997). The

photochemical reaction of PAHs adsorbed to particles could also occur in an organic layer surrounding the particle core (McDow et al., 1994; Ohura et al., 2004, 2005). That is, the direct photolytic pathways of pollutant degradation can be simulated in the laboratory by irradiation of the compound in an organic solvent. The photostability of various PAHs has been investigated in organic solvents such as toluene (Jang and McDow, 1995, 1997), benzene (Jang and McDow, 1997), and cyclohexane (Lamotte et al., 1987).

Environmental occurrences, behavior and toxicity of PAH derivatives have been studied by many researchers. As typical PAH derivatives, nitrated PAHs have been well studied in the fields of environmental behavior because of their high level of toxicity (Finlayson-Pitts and Pitts, 2000). Recently, the focus of attention has been on the effect on the environment of chlorinated polycyclic aromatic hydrocarbons (CIPAHs) with more than 3 rings, which have been found in urban air, snow, tap water, and sediment (Ohura, 2007). Ohura and co-workers

^{*} Corresponding author. Tel.: +81 54 264 5789; fax: +81 54 264 5798.
E-mail address: oura@smail.u-shizuoka-ken.ac.jp (T. Ohura).

(Ohura et al., 2004, 2005; Kitazawa et al., 2006) have detected various CIPAHs associated with particles in urban air, and discussed the fates and possible sources of emission. However, the characteristics of CIPAHs such as environmental fate remain uncertain in comparison with those of the parent PAHs. In this study, we first investigated the photostability of CIPAHs using a chemical model system, followed by comparison to the corresponding parent PAHs. The effects of chlorination of PAHs are discussed on the basis of the photolysis rates and products of each test compound. Note that we used an inert solvent, cyclohexane, for the investigation of photostability to reduce the effects of reactivity of the solvent itself. Finally, the photolysis rate and average quantum yield of each CIPAH and PAH were predicted via a quantitative structure–property relationships (QSPRs) model, which indicated the significant molecular descriptors of the photodegradation.

2. Experimental

2.1. Chemicals

We selected 5 PAH species as reference substances and chlorinated each by the procedure of Dewhurst and Kitchen (1972). The PAHs were selected because of their atmospheric and toxicological relevance. A solution of 20 g of *N*-chlorosuccinimide (Wako Pure Chemical Industries, Ltd., Osaka, Japan) in 20 ml of propylene carbonate (PC, Wako Pure Chemical Industries) and a solution of each PAH (~0.1 M) in 20 ml of PC were mixed and incubated at 100 °C for ~3 h in the dark. The reaction solvent for each PAH was fractionated by high-pressure liquid chromatography (HPLC) (column, COSMOSIL 5C18-AR; eluent, methanol), and the fractions corresponding to the dominant peaks were isolated and analyzed by gas chromatography–mass spectrometry (GC–MS) and by ¹H NMR spectroscopy (500 MHz, CDCl₃), yielding 11 CIPAH

species. The CIPAHs tested in this study are abbreviated as follows: 9-chlorophenanthrene (9-ClPhe), 3,9-dichlorophenanthrene (3,9-Cl₂Phe), 9,10-dichlorophenanthrene (9,10-Cl₂Phe), 3,9,10-trichlorophenanthrene (3,9,10-Cl₃Phe), 3-chlorofluoranthene (3-ClFluor), 8-chlorofluoranthene (8-ClFluor), 3,4-dichlorofluoranthene (3,4-Cl₂Fluor), 3,8-dichlorofluoranthene (3,8-Cl₂Fluor), 1-chloropyrene (1-ClPy), 7-chlorobenz[*a*]anthracene (7-ClBaA), and 6-chlorobenzo[*a*]pyrene (6-ClBaP). The structural formulae of these CIPAHs are illustrated in Fig. 1. The synthesized CIPAHs were >95% pure (as determined by GC–MS).

2.2. Photodegradation experiments

Photodegradation experiments were performed with a turntable photoreactor (Ace Glass Inc., Vineland, NJ) using a 450 W high-pressure mercury lamp (Ushio Co., Ltd., Tokyo, Japan, maximum wavelengths 313, 334, 365, 404, 435, 546, and 578 nm) as the light source, and a quartz immersion well with circulating water. The immersion well was surrounded by a Pyrex sleeve to filter out high-energy UV bands ($\lambda < 290$ nm). Although this setup does not duplicate the spectral distribution of the actinic flux, it does reproduce the wavelengths normally encountered in the atmosphere. The photoreactor was positioned in a water bath with constant water circulation and the temperature in the bath was maintained at 25(±1) °C. The solutions were irradiated in 13 mm × 100 mm quartz reaction tubes.

The quantum yields (ϕ) for each CIPAH and PAH photolysis was determined as follows. The photolysis quantum yield ϕ_{λ_i} for a certain wavelength λ_i (nm) is defined as:

$$\phi_{\lambda_i} = \text{Rate}_{\lambda_i} (I_{\lambda_i}^{\text{abs}})^{-1} \quad (1)$$

where Rate_{λ_i} (mol l⁻¹ s⁻¹) would be the degradation rate of the compound accounted for by the direct photolysis induced by the λ_i emission line only, and $I_{\lambda_i}^{\text{abs}}$ is the intensity of radiation absorption by the compound on irradiation at

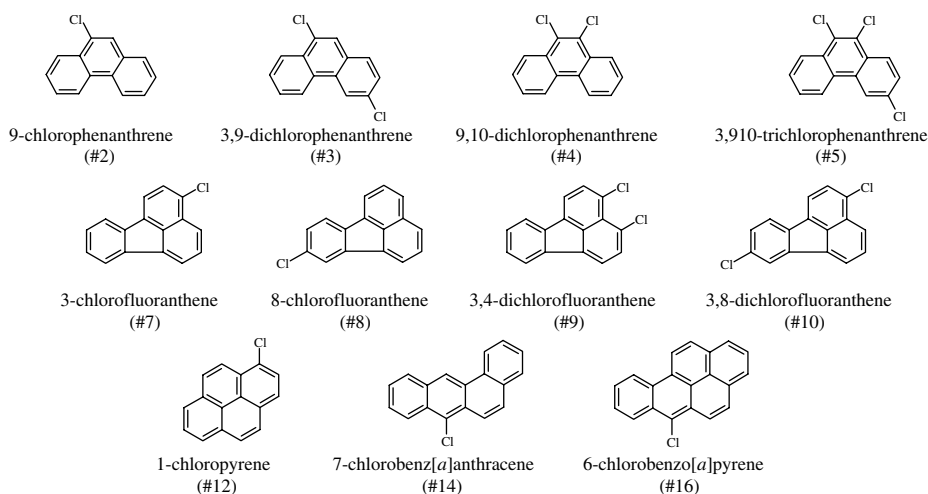


Fig. 1. Chemical structures of the chlorinated polycyclic aromatic hydrocarbons tested (the numbers correspond to those in Table 1).

the wavelength λ_i , which is expressed in equivalent units, $\text{Ein l}^{-1} \text{s}^{-1}$. In the present study, $I_{\lambda_i}^{\text{abs}}$ was observed by using multi channel photo detector (MCPD-3700, Otsuka Electronics, Co. Ltd., Osaka, Japan). The average quantum yields ϕ_{ave} for CIPAH photolysis need to take into account the radiation absorption intensity at the different wavelengths, that is:

$$\begin{aligned} \phi_{\text{ave}} &= \sum_i \frac{I_{\lambda_i}^{\text{abs}}}{I_{\text{tot}}^{\text{abs}}} \phi_{\lambda_i} = \sum_i \frac{I_{\lambda_i}^{\text{abs}}}{I_{\text{tot}}^{\text{abs}}} \frac{\text{Rate}_{\lambda_i}}{I_{\lambda_i}^{\text{abs}}} = \frac{1}{I_{\text{tot}}^{\text{abs}}} \sum_i \text{Rate}_{\lambda_i} \\ &= \frac{\text{Rate}_{\text{Ph}}}{I_{\text{tot}}^{\text{abs}}} \end{aligned} \quad (2)$$

where $\text{Rate}_{\text{Ph}} = \sum_i \text{Rate}_{\lambda_i}$ is the experimentally measured initial degradation rate of each CIPAH on direct photolysis.

Each CIPAH was dissolved in cyclohexane (HPLC grade, Wako Pure Chemical Industries) at a concentration of ~ 0.15 mM. Samples were removed with a pipette, transferred to amber glass chromatography vials, and analyzed with an HP 6890 GC-HP 5972 A MS system in scan mode to identify the photolysis products. The products were analyzed with a DB-5 (5% phenyl-methylpolysiloxane, $60 \text{ m} \times 0.32 \text{ mm} \times 0.25 \mu\text{m}$ film thickness, J&W Scientific) capillary column. Helium was used as the carrier gas at a flow-rate of 1.0 ml min^{-1} . The oven temperature was kept at $80 \text{ }^\circ\text{C}$ for 2 min, then increased from $80 \text{ }^\circ\text{C}$ to $300 \text{ }^\circ\text{C}$ at a rate of $5 \text{ }^\circ\text{C min}^{-1}$, and kept at $300 \text{ }^\circ\text{C}$ for 20 min. The temperature of the injector and GC-MS transfer line was kept at $300 \text{ }^\circ\text{C}$. The MS system was run in the electron impact ionization mode and the electron energy was 70 eV .

2.3. Molecular modeling and statistics

To develop a statistical model, we calculated 8 quantum chemical and geometrical descriptors as follows: the vari-

ous energy levels of the occupied and the unoccupied molecular orbital, for example E_{HOMO} , E_{LUMO} , $E_{\text{HOMO}-1}$, and $E_{\text{LUMO}+1}$, and the related parameters calculated from them, $E_{\text{LUMO}} + E_{\text{HOMO}}$ and $E_{\text{LUMO}} - E_{\text{HOMO}}$, the total energy (TE), and the molecular surface area (SA). All of them were calculated for the optimized molecular structure. Gauss ViewW ver.2.1 (Frisch et al., 2000) was used for three-dimensional molecular modeling of the compounds tested. The molecular structure was optimized by Gaussian 98W ver.5.4 (Frisch et al., 1998). The quantum chemical calculation was performed on the basis of density functional theory in terms of B3LYP as the exchange and the correlation functions and the 3-21* basis set. Next, we selected some significant descriptors, as judged from the values of r^2 , the square of correlation coefficient, and carried out multiple linear regression analysis (MRA) in terms of the descriptors to establish a robust prediction model.

3. Results and discussion

3.1. Photolysis of CIPAHs

The photodegradation of 11 CIPAH congeners and their 5 corresponding parent PAHs were investigated using chemical model systems. Decay of the compounds can be described by the first-order kinetics as follows:

$$\ln(C_t/C_0) = -kt \quad (3)$$

where C_0 and C_t are the concentrations of the compounds at time 0 and at time t , respectively, and k is the photolysis rate constant. The rate constants (k) and half-lives ($t_{1/2}$) estimated from Eq. (3) for degradation of the compounds are given in Table 1. The degradability tended to be higher for relatively high molecular weight (MW) PAHs and CIPAHs, which has also been predicted from the QSPR model of photolysis of PAHs (Chen et al., 2001a,b). As far as the

Table 1
Photolytic kinetic rates and average quantum yields of CIPAHs and the parent PAHs

No.	Compound	Abbreviation	MW ^a	k (h^{-1}) ^b	$t_{1/2}$ (h)	ϕ_{ave}
1	Phenanthrene	Phe	187	0.035	19.7	1.1E-03
2	9-Chlorophenanthrene	9-ClPhe	212	0.089	7.8	2.2E-03
3	3,9-Dichlorophenanthrene	3,9-Cl ₂ Phe	246	0.082	8.5	2.1E-03
4	9,10-Dichlorophenanthrene	9,10-Cl ₂ Phe	246	0.049	14.2	1.1E-03
5	3,9,10-Trichlorophenanthrene	3,9,10-CPhe	280	0.048	14.4	9.0E-04
6	Fluoranthene	Fluor	202	0.031	22.4	3.7E-04
7	3-Chlorofluoranthene	3-ClFluor	236	0.0044	158	6.0E-05
8	8-Chlorofluoranthene	8-ClFluor	236	0.018	38.1	2.9E-04
9	3,4-Dichlorofluoranthene	3,4-Cl ₂ Fluor	270	0.0033	210	5.1E-05
10	3,8-Dichlorofluoranthene	3,8-Cl ₂ Fluor	270	0.0035	198	4.3E-05
11	Pyrene	Py	202	0.203	3.4	5.7E-03
12	1-Chloropyrene	1-ClPy	236	0.315	2.2	6.3E-03
13	Benz[<i>a</i>]anthracene	BaA	228	0.221	3.1	5.4E-03
14	7-Chlorobenz[<i>a</i>]anthracene	7-ClBaA	262	0.104	6.7	2.1E-03
15	Benzo[<i>a</i>]pyrene	BaP	252	1.67	0.4	3.5E-02
16	6-Chlorobenzo[<i>a</i>]pyrene	6-ClBaP	286	0.243	2.9	7.3E-03

^a MW: molecular weight.

^b Data are averages of triplicate experiments.

parent PAHs are concerned, the photostability was as follows; BaP < BaA ≤ Py < Phe < Fluor. This trend is somewhat consistent with the reactivity of PAH toward nitrating species (Nielsen, 1984; Minero et al., 2007) and UV irradiation (Chen et al., 2001a,b). Among the CIPAHs, the rate constant is largest in 1-CIPy, followed by 6-CIBaP, 7-CIBaA, and 9-CIPhe. Although the order of reactivity was somewhat consistent with that of a previous study carried out in toluene (Ohura et al., 2005), the current rate constants were approximately 2–20 times lower than those in the previous study. This difference of reactivity could be due to the hydrogen donor potential of the organic solvents and the stability of the resulting solvent radicals (Dung and O’Keefe, 1994; Ohura et al., 2004).

The rate of photolysis of Phe (Cl = 0) is lower compared to the CIPhe isomers, among which 9-CIPhe was the less photostable compound. Actually, photostability tended to increase again for Cl > 1. Also 1-CIPy showed a photodegradation rate 1.6 times higher compared to the parent PAH. In contrast, among the ClFluor isomers, the photolysis rates decreased with increasing chlorination extent. Also 7-CIBaA and 6-CIBaP were more stable than the parent PAHs. It suggests that certain polycyclic aromatics would be stabilized upon chlorination. Indeed, such stabilization of chlorine-substituted aromatics has been observed in the case of chlorinated dioxins (Kim and O’Keefe, 2000).

Next, to invoke the contribution of different structural features to explain their different behavior, the photolysis quantum yields for the CIPAHs and PAHs were also evaluated. The average quantum yields (ϕ_{ave}) of each compound upon irradiation in cyclohexane are given in Table 1. The order of values calculated were consistent with the corresponding photolysis rate constants, as shown in the highest and lowest value for BaP and 3,8-Cl₂Fluor, respectively.

3.2. Photoproducts

The identification of the important photolytic reactions of pollutants is necessary for the assessment of their hazard for human health and the environment in general. The phototoxicity of many PAHs, including the toxicity of photolytic products, have been observed in various *in vitro* and *in vivo* assays (Arfsten et al., 1996; Yu, 2002; Yan et al., 2004). Therefore, we identified the photolytic products of CIPAHs using GC–MS analysis.

There was no detection of photoproducts from chlorinated derivatives of Fluor, Py, and BaP, suggesting the rapid elimination of these photoproducts upon photolysis. Here, the photoproducts of CIPhes were further investigated. Upon CIPhes photolysis, either oxidized aromatics (fluorenone (Flu) and benzocoumarin (BC)) or their chlorinated derivatives (Cl-Flu and Cl-BC) were tentatively identified as the major photoproducts (Fig. 2a). For 9-CIPhe (compound #2), BC was produced preferentially in comparison to Flu, levels of which were shown as relative intensity to internal standard (Perylene), and built up over

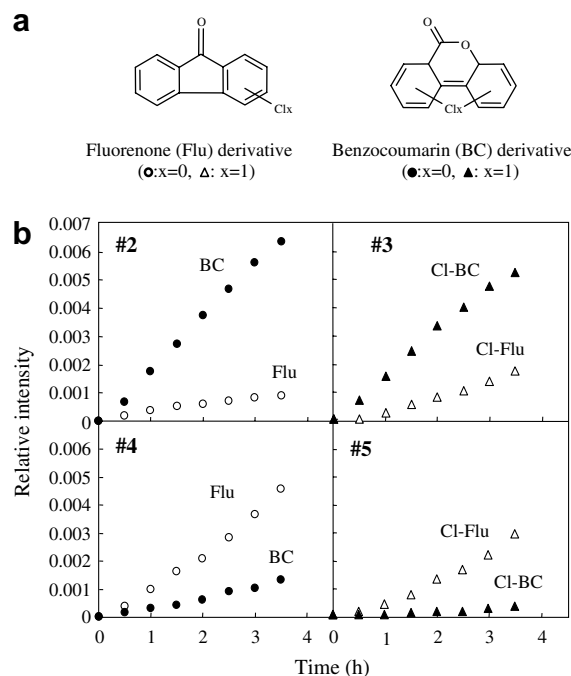


Fig. 2. Photoproducts of chlorinated phenanthrenes produced during the irradiation: (a) chemical structures of fluorenone (Flu) and benzocoumarin (BC) derivatives; (b) production of Flu and BC derivatives in the experiment with 9-CIPhe (#2), 3,9-Cl₂Phe (#3), 9,10-Cl₂Phe (#4), and 3,9,10-Cl₃Phe (#5). Open and closed circles, open and closed triangles show Flu and BC, and chlorinated Flu and BC, respectively.

time (Fig. 2b). Similarly, the photolysis of 3,9-Cl₂Phe (#3) yielded the chlorinated derivative of BC (Cl-BC) as the predominant product. On the other hand, 9,10-Cl₂Phe (#4) and 3,9,10-Cl₃Phe (#5) yielded Flu and the chlorinated derivatives (Cl-Flu) as the predominant products, respectively. As a common feature of CIPhes, those substituted by chlorine at 9 position resulted in production of mainly BC derivatives. Conversely, when the 9 and 10 positions on the Phe are occupied by chlorine, the related CIPhes produce mainly Flu derivatives. Among the photolysis rates of CIPhes, those of 9-CIPhe (#2; $k = 0.089$, see Table 1) and 3,9-Cl₂Phe (#3; 0.082) were approximately 2-fold faster than 9,10-Cl₂Phe (#4; 0.049) and 3,9,10-Cl₃Phe (#5; 0.048). Lee et al. (2001) reported that PAHs are susceptible to oxidation at the position in which frontier electron density is high. Therefore we suggest that oxidation of CIPhes through photolysis occurs preferentially at positions of the highest frontier electron density (9 and 10) compared to abstraction of chlorine from other positions.

3.3. Prediction of photolysis of CIPAHs

To establish quantitative structure–property relationships (QSPRs), a model based on the descriptors derived from quantum computation has been used to predict the direct photolysis of various organic compounds (Chen et al., 1996, 2000, 2001a,b; Sabljic and Peijnenburg, 2001;

Niu et al., 2006). Here, we have developed a QSPR model to estimate the photolytic half-lives and average quantum yields of CIPAHs and PAHs, and then used quantum chemical descriptors with multiple linear regression analysis (MRA) to identify the dominant effects on the photodegradation.

The values of the selected molecular descriptors of each CIPAH and corresponding parent PAH used are summarized in Table 2. To estimate $\log t_{1/2}$ values from those descriptors using MRA, E_{LUMO} , $E_{\text{LUMO}} - E_{\text{HOMO}}$, $E_{\text{LUMO}+1}$, total energy (TE), and surface area (SA) were selected (Table 3), and the analytical QSPR equation for $\log t_{1/2}$ can be obtained and defined as follows:

$$\log t_{1/2} = 125E_{\text{LUMO}} + 24.6(E_{\text{LUMO}} - E_{\text{HOMO}}) + 312E_{\text{LUMO}+1} - 0.00457\text{TE} + 0.00557\text{SA} - 6.90 \quad (4)$$

Furthermore, average quantum yields (ϕ_{ave}) of CIPAHs and PAHs were also predicted from those descriptors using MRA. E_{LUMO} , $E_{\text{LUMO}} - E_{\text{HOMO}}$, and total energy (TE) were selected as the significant descriptors (Table 3), and the QSPR equation for $\log \phi_{\text{ave}}$ can be defined as follows:

$$\log \phi_{\text{ave}} = 119E_{\text{LUMO}} - 71.9(E_{\text{LUMO}} - E_{\text{HOMO}}) - 0.00109\text{TE} + 14.0 \quad (5)$$

The descriptor $E_{\text{LUMO}} - E_{\text{HOMO}}$ is one of the significant factors affecting $\log \phi_{\text{ave}}$ of the CIPAHs and PAHs, and an increase of those values could lead to decrease of $\log \phi_{\text{ave}}$. Chen et al. (2000) also reported that large $E_{\text{LUMO}} - E_{\text{HOMO}}$ is one of the significant descriptors to control the photolysis quantum yields of PAHs. In addition, Pearson (1986) reported that absolute hardness can be expressed as $-(E_{\text{LUMO}} - E_{\text{HOMO}})/2$, which is regarded as a measure of energy stabilization in a chemical system, indicating that chemical structures of molecules tend to be more stable at higher values of $E_{\text{LUMO}} - E_{\text{HOMO}}$ (Niu et al., 2007).

The descriptors $E_{\text{LUMO}+1}$, TE and SA were inter-correlated with each other (Table 4), suggesting that these parameters could play an important role in predicting $\log t_{1/2}$ as shown in Eq. (4). On the other hand, there was little correlation between the three parameters and $E_{\text{LUMO}} - E_{\text{HOMO}}$ (also E_{LUMO}). However, to construct an effective model for predicting $\log \phi_{\text{ave}}$, $E_{\text{LUMO}} - E_{\text{HOMO}}$ and E_{LUMO} should

Table 2
The quantum chemical descriptors for CIPAHs and PAHs used in this study

No. ^a	Descriptors							
	E_{HOMO} (eV)	E_{LUMO} (eV)	$E_{\text{LUMO}} + E_{\text{HOMO}}$ (eV)	$E_{\text{LUMO}} - E_{\text{HOMO}}$ (eV)	$E_{\text{HOMO}-1}$ (eV)	$E_{\text{LUMO}+1}$ (eV)	Total energy (hartree)	Surface area (Å ²)
1	-0.212	-0.0375	-0.249	0.174	-0.223	-0.0312	-540	280
2	-0.218	-0.0477	-0.265	0.170	-0.230	-0.0387	-999	305
3	-0.221	-0.0549	-0.276	0.167	-0.239	-0.0477	-1460	334
4	-0.223	-0.0555	-0.278	0.167	-0.234	-0.0440	-1460	326
5	-0.226	-0.0625	-0.289	0.164	-0.243	-0.0527	-1920	354
6	-0.213	-0.0657	-0.279	0.148	-0.219	-0.0187	-616	289
7	-0.218	-0.0739	-0.292	0.144	-0.223	-0.0259	-1080	316
8	-0.218	-0.0724	-0.291	0.146	-0.224	-0.0278	-1080	323
9	-0.219	-0.0808	-0.300	0.139	-0.226	-0.0332	-1540	339
10	-0.222	-0.0803	-0.302	0.141	-0.230	-0.0341	-1540	349
11	-0.197	-0.0555	-0.253	0.141	-0.229	-0.0238	-616	276
12	-0.202	-0.0633	-0.265	0.138	-0.237	-0.0321	-1080	306
13	-0.197	-0.0580	-0.255	0.139	-0.220	-0.0339	-693	336
14	-0.202	-0.0671	-0.269	0.135	-0.226	-0.0403	-1150	357
15	-0.189	-0.0650	-0.254	0.124	-0.224	-0.0322	-769	329
16	-0.194	-0.0733	-0.267	0.120	-0.230	-0.0381	-1230	353

^a The numbers correspond to those in Table 1.

Table 3
Model fitting results

Variable	$\log t_{1/2}$ (Pred.)			$\log \phi_{\text{ave}}$ (Pred.)		
	Coefficient	SE ^c	P	Coefficient	SE ^c	P
E_{LUMO}	125	82.4	1.6E-01	119	14.0	2.0E-06
$E_{\text{LUMO}} - E_{\text{HOMO}}$	24.6	17.7	1.9E-01	-71.9	9.13	4.4E-06
$E_{\text{LUMO}+1}$	312	112	2.0E-02			
TE ^a	-0.00457	0.0020	4.9E-02	-0.00109	0.00030	3.8E-03
SA ^b	0.0557	0.020	2.1E-02			
Constant	-6.90	4.01	1.2E-01	14.0	1.91	9.4E-06

^a TE: total energy.

^b SA: surface area.

^c SE: standard error.

Table 4
Correlation coefficients between certain quantum chemical descriptors

	E_{LUMO}	$E_{\text{LUMO}} - E_{\text{HOMO}}$	$E_{\text{LUMO}+1}$	TE ^a	SA ^b
E_{LUMO}	1.000				
$E_{\text{LUMO}} - E_{\text{HOMO}}$	0.679	1.000			
$E_{\text{LUMO}+1}$	-0.167	-0.354	1.000		
TE ^a	0.426	-0.142	0.734	1.000	
SA ^b	-0.556	-0.329	-0.643	-0.724	1.000

^a TE: total energy.

^b SA: surface area.

be further added to the prediction parameters as shown in Eq. (5). Therefore, $t_{1/2}$ is mainly influenced by the geometrical characteristics, such as molecular surface area, of the reaction molecules, and ϕ_{ave} may be influenced by the geometrical characteristics as well as the energies of molecular orbitals of the molecules.

In addition, the predicted $\log t_{1/2}$ and $\log \phi_{\text{ave}}$ values were compared to the corresponding observed values

(Table 5). The relationship for $\log t_{1/2}$ values showed significant correlation ($R = 0.951$, Fig. 3a). Similarly, the predicted quantum yields were also closed to the experimental ones ($R = 0.939$, Fig. 3b). It can be concluded that those models can be used to make predictions for other CIPAH congeners, and the prediction may give an initial estimation of photodegradability of the atmospheric CIPAH congeners.

Table 5
Comparison between experimental and predicted $\log t_{1/2}$ or $\log \phi_{\text{ave}}$ values of the CIPAHs and PAHs

No. ^a	$\log t_{1/2}$ (Obs.)	$\log t_{1/2}$ (Pred.)	Diff. ^b	$\log \phi_{\text{ave}}$ (Obs.)	$\log \phi_{\text{ave}}$ (Pred.)	Diff. ^b
1	1.30	1.06	0.24	-2.97	-2.43	-0.54
2	0.893	0.838	0.06	-2.65	-2.83	0.18
3	0.927	0.747	0.18	-2.68	-2.95	0.27
4	1.15	1.37	-0.22	-2.98	-3.06	0.09
5	1.16	1.39	-0.23	-3.05	-3.16	0.12
6	1.35	1.63	-0.28	-3.43	-3.79	0.36
7	2.20	1.83	0.37	-4.22	-3.99	-0.23
8	1.58	1.88	-0.30	-3.53	-3.98	0.44
9	2.32	1.96	0.37	-4.29	-3.94	-0.35
10	2.30	2.41	-0.11	-4.37	-4.07	-0.30
11	0.534	0.433	0.10	-2.24	-2.14	-0.11
12	0.342	0.544	-0.20	-2.20	-2.34	0.14
13	0.496	0.576	-0.08	-2.27	-2.15	-0.12
14	0.823	0.645	0.18	-2.69	-2.44	-0.24
15	-0.381	-0.148	-0.23	-1.46	-1.83	0.37
16	0.456	0.288	0.17	-2.14	-2.07	-0.07

^a The numbers correspond to those in Table 1.

^b Difference between the observed and predicted values.

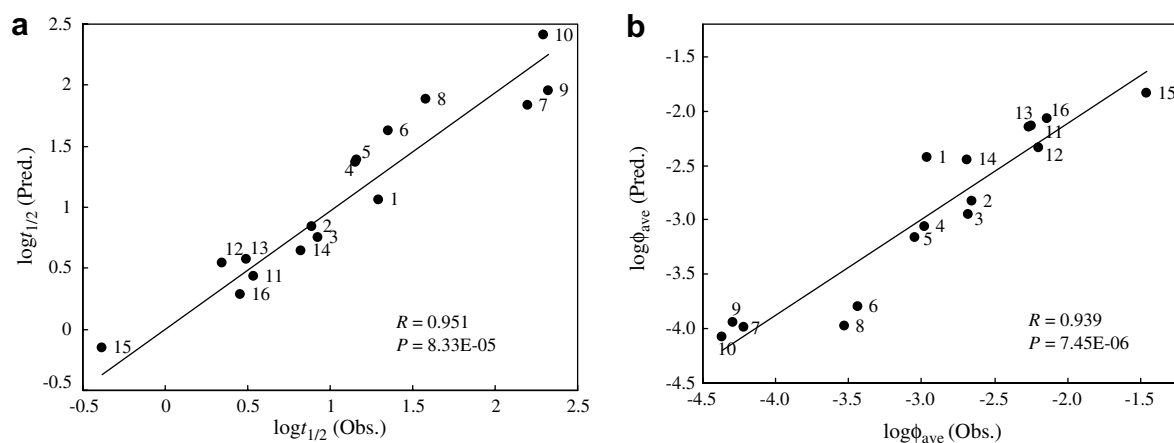


Fig. 3. Plots of observed versus predicted $\log t_{1/2}$ values (a) and $\log \phi_{\text{ave}}$ (b) for CIPAHs and the parent PAHs (the numbers correspond to those in Table 1).

4. Conclusion

For CIPAHs, the photodegradability varied greatly according to the skeleton of PAHs. As far as relatively high-molecular weight PAHs are concerned, such as Fluor, BaA, and BaP, the chloroderivatives were more stable toward photolysis. The photoproducts analysis of CIPes suggested that oxidation occurs at positions of the highest frontier electron density. Furthermore, the QSPR models for direct photolysis half-lives and average quantum yields of 11 CIPAHs and 5 parent PAHs in cyclohexane solution under irradiation by a high-pressure mercury lamp was developed, and shown to have good predictive abilities. The significant factors affecting photolytic half-lives of the compounds were E_{LUMO+1} , total energy, and surface area values, while E_{LUMO} , $E_{LUMO} - E_{HOMO}$, and total energy control the photolysis quantum yields.

Acknowledgements

This work was supported, in part, by a Grant-in-aid for Young Scientists (B) from the Japan Society for the Promotion of Science (Project No. 14780416, to T.O).

References

- Arfsten, D.P., Schaeffer, D.J., Mulveny, D.C., 1996. The effects of near ultraviolet radiation on the toxic effects of polycyclic aromatic hydrocarbons in animals and plants: A review. *Ecotoxicol. Environ. Safe.* 33, 1–24.
- Baek, S.O., Field, R.A., Goldstone, M.E., Kirk, P.W., Lester, J.N., 1991. A review of atmospheric polycyclic aromatic hydrocarbons: Sources, fate and behavior. *Water Air Soil Pollut.* 60, 279–300.
- Bidleman, T.F., 1988. Atmospheric processes, wet and dry deposition of organic compounds are controlled by their vapor-particle partitioning. *Environ. Sci. Technol.* 22, 361–367.
- Chen, J.W., Kong, L.R., Zhu, C.M., Huang, Q.G., Wang, L.S., 1996. Correlation between photolysis rate constants of polycyclic aromatic hydrocarbons and frontier molecular orbital energy. *Chemosphere* 33, 1143–1150.
- Chen, J., Peijnenburg, W.J.G.M., Quan, X., Yang, F., 2000. Quantitative structure-property relationships for direct photolysis quantum yields of selected polycyclic aromatic hydrocarbons. *Sci. Total Environ.* 246, 11–20.
- Chen, J., Quan, X., Schramm, K.-W., Ketttrup, A., Yang, F., 2001a. Quantitative structure-property relationships (QSPRs) on direct photolysis of PCDDs. *Chemosphere* 45, 151–159.
- Chen, J., Quan, X., Yan, Y., Yang, F., Peijnenburg, W.J.G.M., 2001b. Quantitative structure-property relationship studies on direct photolysis of selected polycyclic aromatic hydrocarbons in atmospheric aerosol. *Chemosphere* 42, 263–270.
- Dewhurst, F., Kitchen, D.A., 1972. Synthesis and properties of 6-substituted benzo[a]pyrene derivatives. *J. Chem. Soc. Perk. T 2*, 710–712.
- Dung, M.H., O'Keefe, P.W., 1994. Comparative rates of photolysis of polychlorinated dibenzofurans in organic solvents and in aqueous solutions. *Environ. Sci. Technol.* 28, 549–554.
- Finlayson-Pitts, B.J., Pitts Jr., J.N., 1997. Tropospheric air pollution: Ozone, airborne toxics, polycyclic aromatic hydrocarbons, and particles. *Nature* 276, 1045–1052.
- Finlayson-Pitts, B.J., Pitts Jr., J.N., 2000. *Chemistry of the Upper and Lower Atmosphere*. Academic Press, San Diego.
- Frisch, M.J., Nielsen, A.B., Holder, A.J., 2000. Gauss ViewW User's Reference. Gaussian, Inc., Pittsburgh, PA.
- Frisch, M.J., Trucks, G.W., Schlegel, H.B., Scuseria, G.E., Robb, M.A., Cheeseman, J.R., Zakrzewski, V.G., Montgomery Jr., J.A., Stratmann, R.E., Burant, J.C., Dapprich, S., Millam, J.M., Daniels, A.D., Kudin, K.N., Strain, M.C., Farkas, Ö., Tomasi, J., Barone, V., Cossi, M., Cammi, R., Mennucci, B., Pomelli, C., Adamo, C., Clifford, S., Ochterski, J., Petersson, G.A., Ayala, P.Y., Cui, Q., Morokuma, K., Salvador, P., Dannenberg, J.J., Malick, D.K., Rabuck, A.D., Raghavachari, K., Foresman, J.B., Cioslowski, J., Ortiz, J.V., Baboul, A.G., Stefanov, B.B., Liu, G., Liashenko, A., Piskorz, P., Komáromi, I., Gomperts, R., Martin, R.L., Fox, D.J., Keith, T., Al-Laham, M.A., Peng, C.Y., Nanayakkara, A., Challacombe, M., Gill, P.M.W., Johnson, B., Chen, W., Wong, M.W., Andres, J.L., Gonzalez, C., Head-Gordon, M., Replogle, E.S., Pople, J.A., 1998. Gaussian 98. Gaussian, Inc., Pittsburgh, PA.
- Jang, M., McDow, S.R., 1995. Benz[a]anthracene photodegradation in the presence of known organic constituents of atmospheric aerosols. *Environ. Sci. Technol.* 29, 2654–2660.
- Jang, M., McDow, S.R., 1997. Products of benz[a]anthracene photodegradation in the presence of known organic constituents of atmospheric aerosols. *Environ. Sci. Technol.* 31, 1046–1053.
- Kamens, R.M., Guo, Z., Fulcher, J.N., Bell, D.A., 1988. Influence of humidity, sunlight, and temperature on the daytime decay of polycyclic aromatic hydrocarbons on atmospheric soot particles. *Environ. Sci. Technol.* 22, 103–108.
- Kim, M., O'Keefe, P.W., 2000. Photodegradation of polychlorinated dibenzo-p-dioxins and dibenzofurans in aqueous solutions and in organic solvents. *Chemosphere* 41, 793–800.
- Kitazawa, A., Amagai, T., Ohura, T., 2006. Temporal trends and relationships of particulate chlorinated polycyclic aromatic hydrocarbons and their parent compounds in urban air. *Environ. Sci. Technol.* 40, 4592–4598.
- Lamotte, M., Pereyre, J., Joussot-Dubien, J., Lapouyade, R., 1987. The photolysis of pyrene and perylene in cyclohexane liquid solution from highly excited electronic states. *J. Photochem.* 38, 177–188.
- Lee, B.-D., Iso, M., Hosomi, M., 2001. Prediction of Fenton oxidation positions in polycyclic aromatic hydrocarbons by frontier electron density. *Chemosphere* 42, 431–435.
- Lönnermark, A., Blomqvist, P., 2006. Emissions from an automobile fire. *Chemosphere* 62, 1043–1056.
- Mantis, J., Chaloulakou, A., Samara, C., 2005. PM10-bound polycyclic aromatic hydrocarbons (PAHs) in the Greater Area of Athens, Greece. *Chemosphere* 59, 593–604.
- McDow, S.R., Sun, O.-R., Vartiainen, M., Hong, Y.-S., Yao, Y.-L., Fister, T., Yao, R.-Q., Kamens, R.M., 1994. Effect of composition and state of organic components on polycyclic aromatic hydrocarbon decay in atmospheric aerosols. *Environ. Sci. Technol.* 28, 2147–2153.
- Menzie, C.A., Potocki, B.B., Santodonato, J., 1992. Exposure to carcinogenic PAHs in the environment. *Environ. Sci. Technol.* 26, 1278–1284.
- Minero, C., Bono, F., Rubertelli, F., Pavino, D., Maurino, V., Pelizzetti, E., Vione, D., 2007. On the effect of pH in aromatic photonitration upon nitrate photolysis. *Chemosphere* 66, 650–656.
- Nielsen, T., 1984. Reactivity of polycyclic aromatic hydrocarbons toward nitrating species. *Environ. Sci. Technol.* 18, 157–163.
- Niu, J.F., Shen, Z.Y., Yang, Z.F., Long, X.X., Yu, G., 2006. Quantitative structure-property relationships on photodegradation of polybrominated diphenyl ethers. *Chemosphere* 64, 658–665.
- Niu, J., Wang, L., Yang, Z., 2007. QSPRs on photodegradation half-lives of atmospheric chlorinated polycyclic aromatic hydrocarbons associated with particulates. *Ecotoxicol. Environ. Safe.* 66, 272–277.
- Ohura, T., 2007. Environmental behavior, sources, and effects of chlorinated polycyclic aromatic hydrocarbons. *The Scientific World J.* 7, 372–380.
- Ohura, T., Kitazawa, A., Amagai, T., 2004. Seasonal variability of 1-chloropyrene on a atmospheric particles and photostability in toluene. *Chemosphere* 57, 831–837.
- Ohura, T., Kitazawa, A., Amagai, T., Makino, M., 2005. Occurrence, profiles, and photostabilities of chlorinated polycyclic aromatic

- hydrocarbons associated with particulates in urban air. *Environ. Sci. Technol.* 39, 85–91.
- Pearson, P.G., 1986. Absolute electronegativity and hardness correlated with molecular orbital theory. *Proc. Natl. Acad. Sci.* 83, 8440–8441.
- Pekey, B., Karakaş, D., Ayberk, S., 2007. Atmospheric deposition of polycyclic aromatic hydrocarbons to Izmit Bay, Turkey. *Chemosphere* 67, 537–547.
- Sabljić, A., 2001. QSAR models for estimating properties of persistent organic pollutants required in evaluation of their environmental fate and risk. *Chemosphere* 43, 363–375.
- Sabljić, A., Peijnenburg, W., 2001. Recommendations on modeling lifetime and degradability of organic compounds in air, soil and water systems. *Pure Appl. Chem.* 73, 1331–1348.
- Yan, J., Wang, L., Fu, P.P., Yu, H., 2004. Photomutagenicity of 16 polycyclic aromatic hydrocarbons from the US EPA priority pollutant list. *Mutat. Res.* 557, 99–108.
- Yu, H., 2002. Environmental carcinogenic polycyclic aromatic hydrocarbons: Photochemistry and phototoxicity. *J. Environ. Sci. Heal. C* 20, 149–183.